ECS Transactions, 50 (11) 71-78 (2012)
10.1149/05011.0071ecst ©The Electrochemical Society

An Arrhenius Argument to Explain Electrical Conductivity Maxima versus Temperature

C. M. Kuntz and A. L. L. East

Department of Chemistry and Biochemistry, University of Regina, Regina, Saskatchewan S4S 0A2 Canada

The existence of conductivity maxima in pure molten salt was interpreted by Grantham and Yosim to be due to ion association at low densities. Tödheide used a chloride-transfer shifting-equilibrium hypothesis to explain ion association in the case of bismuth trichloride. We have performed density-functional-theory based molecular dynamics simulations of the molten chlorides of Bi(III), Sn(II), and Hg(II), and Tödheide's hypothesis is not supported. Instead, the simulations imply a hopping barrier for ions between counterions, and we develop this concept into a density-dependent Arrhenius equation to explain the conductivity maxima.

Introduction

Smedley's 1980 text on the ionic conductivity of liquids (1) groups its discussion of molten salt conductivity in a way that parallels changes in Arrhenius behavior. Chapter 3 discusses cases of negative curvature in Arrhenius plots at "low-temperature," which at the time was seen only in molten salt mixtures. Chapter 4 discusses cases of linear Arrhenius plots at "high temperature," defined as temperatures above twice the glass transition temperature ($> 2T_0$). Chapter 5 discusses cases of negative curvature so severe that conductivity maxima are seen; such maxima are thought to occur for "most, if not all" (1) salts if heated to particularly high temperatures, as this was thought to cause "partially ionized" molten salts.

The present report is concerned with these Chapter 5 cases, and the nature of "partial ionization" (or "ion association"). A classic example is that of bismuth trichloride, whose conductivity, viscosity, and Walden plots appear in Figure 1.

In the 1960s, Grantham and Yosim (2-5) studied many maxima-producing melts under orthobaric conditions, and, noting the liquid expansion upon heating, supposed that the loss of conductivity at higher temperatures is due to increased "ion association" as density falls. Tödheide (6,7) hypothesized that, in their classic case ($BiCl_3$), "ion association" was a shift to the left in the equilibrium $2\ BiCl_3 \Leftrightarrow BiCl_2^+ + BiCl_4^-$. Tödheide added a degree of ionization α into the theory, assumed monotonically increasing ion mobilities with temperature, and showed that the conductivity maximum can be explained with α values that steadily decrease as the density falls during orthobaric heating. Since Raman and neutron-scattering studies have been inconclusive on the nature of the ions present (8-11), we recently decided to test Tödheide's hypothesis using computational simulation of molten bismuth trichloride (12). The result was a liquid composed of atomic ions, not the equilibrium Tödheide imagined.

Our $BiCl_3$ simulations at temperatures past T_{max} revealed increasing examples of chloride ion vibrations against a single Bi atom, as opposed to the "bridging-chloride" situations that dominate. The "bridging-chloride" situations also increasingly showed asymmetry, i.e. as if a barrier had formed to impede vibration of Cl from one Bi to the other. Hence we replaced Tödheide's explanation of "ion association" with an activation energy explanation: the activation energy for the conductivity process is the barrier, principally Coulombic, for an ion to hop from counterion to counterion, a barrier which increases as density falls because the average distance between counterions increases. A density-dependent Arrhenius equation fit the experimental conductivities splendidly, and could also explain the results of two simulations under "off-diagonal" conditions (high T with high ρ, and low T with low ρ) as well (12).

This report presents our results from simulations of other molten salts to further test the density-dependent-Arrhenius idea. Our earlier discussion (12) of other modified Arrhenius relations, including the Vogel-Fulcher-Tammann equation, will be reiterated here as well.

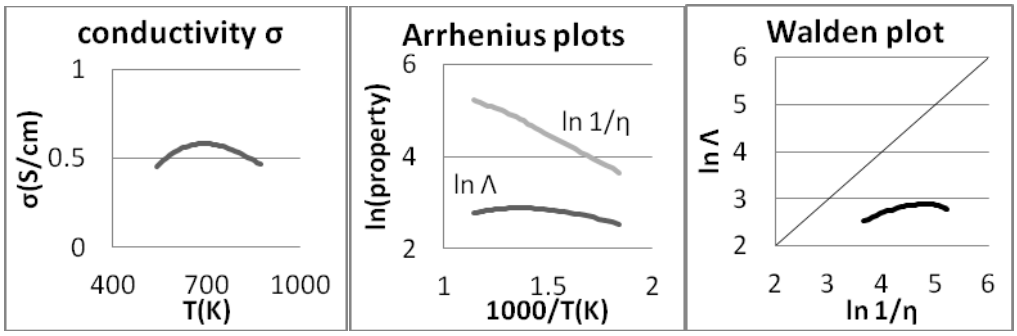

Figure 1. Plots of experimental data for molten $BiCl_3$. Viscosities η are from Kellner (13); conductivities σ and densities (for deriving molar conductivities Λ) are from Janz (14). Units: Poise for η, and S cm^2 per mole of unit charge for Λ.

Methodology

Simulations were performed as before (12) using the Vienna Ab-initio Simulation Package (VASP) software (15,16), using its potpawGGA plane-wave basis sets (17,18), standard precision (PREC = NORMAL), ENMAX = 400 eV, a Nosé thermostat for canonical-ensemble (NVT) conditions (19) with 40 fs thermal oscillations (SMASS = 0), and a Verlet velocity algorithm (20) with timestep $\tau = 4$ fs. For forces, the PW91 level of density functional theory (21) was used with an added, Grimme-style (22), semiempirical van-der-Waals (vdW) attractive potential, as before (12). For Hg the Grimme parameters were taken to be $C_6 = 42.807$ J nm^6 mol^{-1} and $R_0 = 1.6$ Å; the former was calculated using the same UPBE0/QZVP recipe Grimme used, and the latter was taken to be the same as Grimme used for Cd, the element above it in the periodic table, due to the lanthanide contraction rule.

The simulations of $SnCl_2$ and $HgCl_2$ used a cubic simulation cell of $M_{40}Cl_{80}$ (M = Hg or Sn) which was replicated using periodic boundary conditions to mimic the bulk liquid.

After 7100 timesteps (28.4 ps) for equilibration, the simulations ran for 25000 steps ($HgCl_2$) or 50000 steps ($SnCl_2$) for sampling. The longer simulations for $SnCl_2$ were to improve the statistical precision of the conductivity calculation in an unsuccessful attempt to observe the conductivity maximum. Cell widths were chosen to match the liquid density appropriate for the temperature simulated; these densities (g mL^{-1}) were computed from formulae summarized by Janz (14):

$$\rho\ (SnCl_2) = 4.016 - 0.001253\ T\ (K) \quad [1]$$
$$\rho\ (HgCl_2) = 5.9391 - 0.0028624\ T\ (K) \quad [2]$$

A table of such widths and densities appear in Table I.

TABLE I. Densities[a] and Simulation Cell Parameters.

Liquid	ρ_{mass} (g mL^{-1})	$\rho_{cations}$ ($Å^{-3}$)	Atoms/cell	Cell width (Å)
$HgCl_2$ (560 °C)	3.5543	0.00788	120	17.18
$SnCl_2$ (560 °C)	2.9721	0.00944	120	16.18
$BiCl_3$ (580 °C)	3.1108	0.00594	64[b]	13.91[b]

[a] Mass densities taken from Janz (14). [b] Ref. 12.

Computation of transport properties were done via Einstein formulae as described before (12), except for the $HgCl_2$ case in which extrapolations to $t \rightarrow \infty$ were performed via least-square fits of all data past t = 11.6 ps to the exponential decay equation $a + b\ e^{-ct}$.

Results

Specific Conductivity and Diffusion Constants. Table II reports our results for selected transport properties. While the chlorides of Bi(III) and Sn(II) are truly molten salts, that of Hg(II) is a molecular liquid of limited conductivity; it was chosen as an example of asymptotically complete "ion association." The conductivity predictions are in qualitative agreement with experiment, lending faith in the simulations; the remaining error is largely due to imprecise statistics, rather than the approximation used for forces in the simulations. The high diffusion constant of the heavy mercury ions is due to the molecular nature of $HgCl_2$; since Hg and Cl ions travel together in this liquid, their D values must be similar. Chloride diffusion is roughly but not quite the same for each liquid, *despite the wide range of conductivities*. This is because diffusion relates to absolute mobility, whereas conductivity relates to relative mobility versus counterions, and "ion association" can reduce relative mobility far more significantly than absolute mobility. As another example of this distinction, for $BiCl_3$ we found diffusion constants to continually increase with temperature, unlike the conductivity which rises and then falls (12).

TABLE II. Specific Conductivities σ (S cm^{-1}) and Diffusion Constants D (10^{-10} $m^2\ s^{-1}$) from Simulation.

Liquid	σ	σ_{expt}	D(cation)	D(Cl)
$HgCl_2$ (560 °C)	0.008	0.00008[b]	56.6	58.8
$SnCl_2$ (560 °C)	2.5	2.33[c]	33.9	51.1
$BiCl_3$ (580 °C)[a]	1.8	0.49[d]	37.9	61.2

[a] Ref. 12. [b] Cubic extrapolation of Ref. 3 data. [c] Linear interpolation of Ref. 3 data. [d] Linear interpolation of Ref. 2 data.

Radial Distribution Functions g(r). The radial distributions of Cl about each cation (Figure 2) clearly demonstrate the difference between molecular liquid $HgCl_2$ versus true molten salts $SnCl_2$ and $BiCl_3$. The latter show broad peaks from 2.4-4.0 Å containing roughly 6 bridging chloride ions, while for $HgCl_2$ this peak is split into 2 well-defined peaks of singly-coordinate Cl^-. The reason for $HgCl_2$ being molecular is a ~ 100 kJ mol^{-1} additional covalent binding effect: quantum chemistry predictions of the MCl_2 (g) → M^{2+} (g) + 2 Cl^- (g) binding energies are 1991 vs. 1895 kJ mol^{-1} for Hg vs Sn (23). Importantly, the Tödheide structural hypothesis of molecules and molecular ions for molten $BiCl_3$ is not supported, since such a hypothesis would require of g(r) a separation of covalent (2.3-2.5 Å) and next-nearest (3-4 Å) chlorides as in the $HgCl_2$ case.

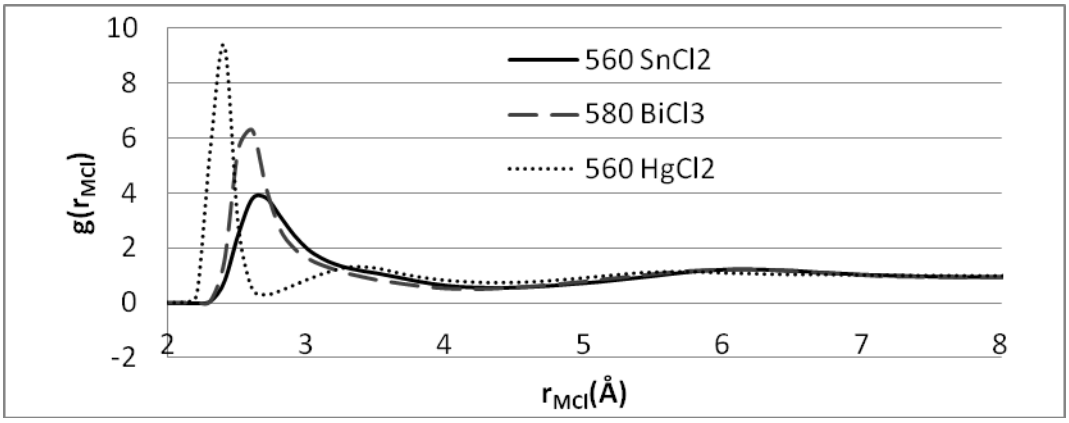

Figure 2. Radial distribution plots of Cl atoms from a metal atom, in three liquid chlorides as computed from simulations. $HgCl_2$, an essentially molecular liquid, features two covalent chlorides (r = 2.4 Å) and no bridging chlorides (2.6-2.9 Å), unlike $SnCl_2$ and $BiCl_3$.

With the $HgCl_2$ as an example of asymptotically complete "ion association," we revisit the g(r) results for $BiCl_3$ at varying temperatures (Figure 3). As the temperature is raised (and the density correspondingly lowered), g(r) shows smooth, gradual evolution towards the $HgCl_2$-like example, i.e. an increase in "ion association."

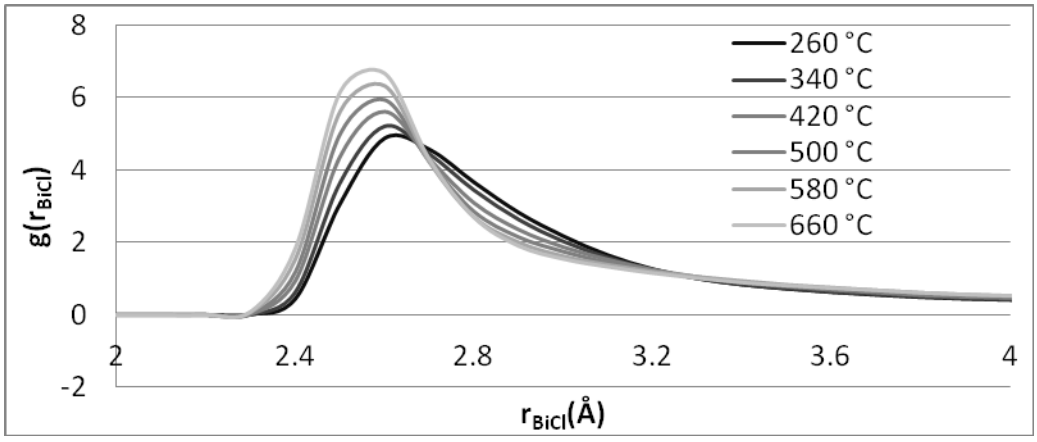

Figure 3. Radial distribution plots of Cl atoms from Bi atom, in molten $BiCl_3$ simulations. Data from simulations of ref. 12.

We feel that the new results for $SnCl_2$ and $HgCl_2$ support our earlier claim (12) that the increased "ion association" that produces conductivity maxima is due to a gradually rising energy barrier for ions to hop from counterion to counterion, and not a thermodynamic equilibrium shift from molecular ions to neutral molecules via halide-ion transfer. The increase in the counterion-to-counterion hopping barriers is due to increased counterion-counterion distance, which is due to the lowered density, which itself is caused by the larger atomic vibrational amplitudes afforded by increased temperature.

Discussion

Given the new hypothesis that a rising barrier for ion hopping is the reason for the apparent increased degree of ion association that causes conductivity maxima at elevated temperatures, one is naturally led to considering activation energy theories, and the various modified Arrhenius relations that have been proposed for transport properties. Some examples are shown in Equations 3-6.

$$y_{ARR} = Ae^{B/RT} \quad \text{(Arrhenius)} \quad [3]$$

$$y_{LIT} = Ae^{B/RT^3} \quad \text{(Litovitz)} \quad [4]$$

$$y_{VFT} = Ae^{B/R(T-T_0)} \quad \text{(Vogel-Fulcher-Tammann)} \quad [5]$$

$$y_{DOR} = A_1e^{B_1/RT} + A_2e^{B_2/RT} \quad \text{(Doremus)} \quad [6]$$

All A and B are assumed constants. The Litovitz and VFT (Vogel-Fulcher-Tammann) equations have been used for both conductivity and viscosity by Harris, Kanakubo, and co-workers for modern ionic liquids (24). The Doremus function is newest and was used to explain the viscosity of silica, which in an Arrhenius plot appears to have a kink separating two linear regions of differing slopes (25,26).

The fundamental problem with the Litovitz and VFT equations for conductivity-maximum cases is that they cannot produce a maximum. The Doremus function can produce a maximum, but in an Arrhenius plot it appears as a kink between two linear regions. As can be seen in the Arrhenius plots of Figure 1, the fluidity (and hence viscosity) of $BiCl_3$ does indeed show such behavior, but the conductivity of $BiCl_3$ does not. Is yet another modified Arrhenius equation needed?

We are currently of the mind that non-Arrhenius behavior might generally be handled by considering indirect temperature dependence of the two Arrhenius parameters in the original Arrhenius function (ARR, eq. 3). Given a fixed number of moles of a substance, a 3-variable equation of state like $\rho = f(p,T)$ has two independent variables, but often p is determined by experimental conditions (e.g. atmospheric pressure, orthobaric conditions…), so that

$$\rho_{expt} = f(T) \quad [7]$$

If one considers the Arrhenius parameters to be *density-dependent* (ARRD):

$$y_{ARRD} = A(\rho)e^{-E_a(\rho)/RT} \quad [8]$$

then, in constant-density (constant-volume) conditions, temperature dependence of the transport property should have perfect Arrhenius behavior (ln y versus 1/T perfectly linear), but in other conditions where Eq. 7 holds, the Arrhenius parameters A and E_a have indirect temperature dependence and "non-Arrhenius" behavior will occur.

Equation 8 was shown (12) to fit the true maximum-possessing $BiCl_3$ conductivity curve by considering a simple two-parameter linear relation for the prefactor A(ρ), and a straightforward one-parameter function for $E_a(\rho)$ derived from intersecting -1/r Coulombic attractive potentials for an ion to two counterions on either side:

$$A(\rho) = A_0 - A_1\rho \quad [9]$$

$$E_a(\rho) = \frac{|q_1 q_2|}{4\pi\varepsilon_0}\left(\frac{R}{r_0(R-r_0)} - \frac{4}{R}\right),\ R \geq 2r_0 \quad [10]$$

In Eq. 10, R is the counterion-counterion distance and r_0 is the preferred cation-anion distance, taken from radial distribution plots. Eq. 10 is dependent upon density because $R = P\rho^{-1/3}$ for some proportionality parameter P. E_a is zero when the anion is in contact with both cations ($R = 2r_0$), and E_a approaches its asymptotic maximum $E_{a,max} = |q_1 q_2|/4\pi\varepsilon_0 r_0$ as $R \rightarrow \infty$, i.e. as $\rho \rightarrow 0$. For $BiCl_3$, $q_1 = 3e$, $q_2 = -e$, $r_0 = 2.6$ Å (Fig. 3), and $E_{a,max} = 1603$ kJ mol^{-1}, and after fitting, $A_0 = 4.012$ S cm^{-1}, $A_1 = 0.9306$ S cm^2 g^{-1}, and P = 8.18 Å g$^{1/3}$ cm.

We moved on to apply Eqs. 8-10 to the maxima-containing experimental conductivities of other liquids, but had less success. One issue is that Eq. 10 is purely Coulombic and does not take into account any covalent interactions. Work is still required to develop more universal functions for Eqs. 9-10. To gain a better idea for the terms needed to improve the $E_a(\rho)$ expression, a crude flux theory for A(ρ) was derived, and plots of $E_a(\rho)$ were then derived from these A values and experimental conductivities. This work is described below.

A(ρ) should be the equivalent conductivity σ(ρ,T) if there were no activation energy for the process (E_a=0). Hence, the directional flow of anions to an electrode would only be limited by collisions against oncoming cations. Using a computation of the density-dependent probability than an ion collides with a counterion when travelling through a slab of space of width 2r (r = radius of counterion), the result is a linear function of density:

$$A(\rho) = (1 - 2\pi r_+^3\rho_+)A_{0,-} + (1 - 2\pi r_-^3\rho_-)A_{0,+} \quad [11]$$

In lieu of a better idea, both A_0 values have been arbitrarily set at 4 S cm^{-1} for each of the 6 liquids in our training set; this is the lowest common integer value for which all E_a values of highly-conducting CuCl remain positive. The radii used were Shannon-Prewitt crystal radii for 6-coordinate ions (27,28), and number densities of ions are easily derived from the mass density ρ and stoichiometry.

From Eq. 8, using experimental conductivities for y_{ARRD}, prefactors A(ρ) from Eq. 11, and densities from the linear functions of Janz (14), $E_a(T)$ functions were derived and plotted in Figure 4. The two low-conducting mercuric halides produce large hopping activation energies, forcing essentially complete "ion association" into molecules. The highly conducting CuCl has very low E_a values which slightly rise as the liquid expands with temperature. Most interestingly, for the other three molten salts ($BiCl_3$, $SnCl_2$, ZnI_2), the E_a curves have minima. Perhaps conductivity is hindered not only by a hopping barrier that indirectly rises with T, but some additional barrier that indirectly falls with T. Such a barrier might arise for an ion squeezing through tightly-packed regions, for instance.

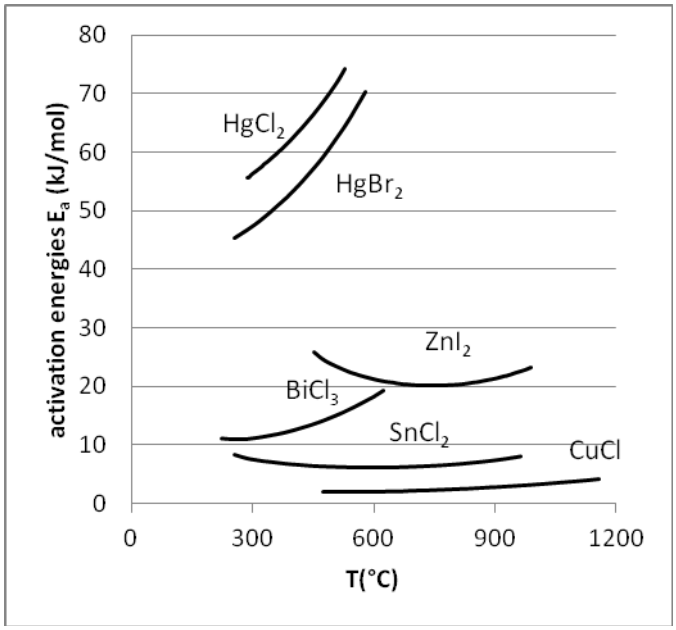

Figure 4. Activation barriers for ion hopping in various liquid halides, as indirect functions of temperature. Derived from experimental conductivities from Refs. 2 ($BiCl_3$) and 3 (all others).

Conclusions

New simulations on molten $SnCl_2$ and $HgCl_2$ lend further support to the hypothesis that "ion association" is due to an activation energy barrier for the hopping of an ion from counterion to counterion. This barrier rises as density falls, and therefore indirectly rises as temperature rises in experiments like those of Grantham and Yosim. A density-dependent Arrhenius equation shows promise in reproducing such maxima from the hopping-barrier idea, but more theoretical work is needed. From a crude flux theory for the Arrhenius prefactor A(ρ), activation energies E_a for the process of conductivity were derived for 6 liquid halides, and resulted in the interesting possibility that E_a is the sum of two terms, the second being a term that recedes as density falls.

Acknowledgments

The Natural Sciences and Engineering Research Council (Canada) is thanked for operational funding, and the Laboratory of Computational Discovery (Regina) for supercomputer support. K. E. Johnson (Regina) is thanked for valuable discussions.

References

1. S. I. Smedley, *The Interpretation of Ionic Conductivity in Liquids*, Plenum Press, New York (1980).
2. L. F. Grantham and S. J. Yosim, *J. Phys. Chem.* **67**, 2506 (1963).
3. L. F. Grantham and S. J. Yosim, *J. Chem. Phys.* **45**, 1192 (1966).
4. L. F. Grantham and S. J. Yosim, *J. Phys. Chem.* **72**, 762 (1968).
5. A. J. Darnell, W. A. McCollum, and S. J. Yosim, *J. Phys. Chem.* **73**, 4116 (1969).
6. G. Treiber and K. Tödheide, *Ber. Bunsenges. Phys. Chem.* **77***,* 540 (1973).
7. K. Tödheide, *Angew. Chem. Int. Ed. Engl.* **19**, 606 (1980).
8. J. T. Kenney and F. X. Powell, *J. Phys. Chem.* **72**, 3094 (1968).
9. E. Denchik, S. C. Nyburg, G. A. Ozin, and J. T. Szymanski, *J. Chem. Soc. A* 3157 (1971).
10. K. W. Fung, G. M. Begun, and G. Mamantov, *Inorg. Chem.* **12**, 53 (1973).
11. D. L. Price, M.-L. Saboungi, W. S. Howells, and M. P. Tosi, in *Proc. Int. Symp. Molten Salts,* M.-L. Saboungi et al., Editors, PV 93-9, p. 1, The Electrochemical Society Proceedings Series, Pennington, N. J. (1993).
12. A. T. Clay, C. M. Kuntz, K. E. Johnson, and A. L. L. East, *J. Chem. Phys.* **136**, 124504 (2012).
13. J. D. Kellner, *J. Phys. Chem.* **72**, 1737 (1968).
14. G. J. Janz, *J. Phys. Chem. Ref. Data* **17**, Supplement No. 2 (1988).
15. G. Kresse and J. Hafner, *Phys. Rev. B* **47**, 558 (1993).
16. G. Kresse and J. Furthmüller, *Phys. Rev. B* **54**, 11169 (1996).
17. G. Kresse and J. Hafner, *J. Phys. Condens. Matter* **6**, 8245 (1994).
18. G. Kresse and D. Joubert, *Phys. Rev. B* **59**, 1758 (1999).
19. S. Nosé, *J. Chem. Phys.* **81**, 511 (1984).
20. A. R. Leach, *Molecular Modelling: Principles and Applications*, 2nd ed., Pearson, Harlow, UK (2001).
21. J. P. Perdew, J. A. Chevary, S. H. Vosko, K. A. Jackson, M. R. Pedersen, D. J. Singh, and C. Fiolhais, *Phys. Rev. B* **46**, 6671 (1992).
22. S. Grimme, *J. Comp. Chem.* **27**, 1787 (2006).
23. From B3LYP/LANL2DZ electronic energies computed with Gaussian09 software (Gaussian, Inc.; Wallingford, CT).
24. K. R. Harris, M. Kanakubo, N. Tsuchihashi, K. Ibuki, and M. Ueno, *J. Phys. Chem. B* **112**, 9830 (2008), and references therein.
25. R. H. Doremus, J. App. Phys. **92**, 7619 (2002).
26. Doremus (ref. 24) wrote his equation as $\eta = Ae^{B/RT}[1 + Ce^{D/RT}]$, which is equivalent to Eq. 6 if $A_1 = A$, $A_2 = AC$, $B_1 = B$, and $B_2 = B+D$.
27. R. D. Shannon, *Acta Cryst* **A32**, 751 (1976).
28. For Sn(II) a value of 1.16 was derived from interpolation of values for Ge(II) and Pb(II), using the interpolation ratio (Sn-Pb)/(Ge-Pb) observed for the IV oxidation state.